Review Article

Rik Jonckheere*

EUV mask defectivity – a process of increasing control toward HVM

DOI 10.1515/aot-2017-0017
Received March 6, 2017; accepted April 19, 2017

Abstract: This article covers the various aspects of defectivity of a typical mask used for extreme ultra-violet (EUV) lithography. The focus of the present article is on those aspects that are more specific for EUV lithography. A prime type of defect that fully falls under the really EUV-specific category consists of the so-called multilayer defects (ML-defects): these defects relate to the ML mirror on the mask, which makes it reflective. While not specific, particle contamination plays a special role in EUV lithography and includes two aspects: both front- and backside of an EUV mask have peculiarities beyond historical deep-UV lithography. Frontside particles can print when they exceed a critical size and, while solvable as in (deep)-UV lithography by means of a pellicle, there are specific challenges. Backside particles can distort a clamped EUV reticle, and the resulting local non-flatness of the reticle may result in focus and overlay errors on the wafer. A last aspect that requires special attention for EUVL can be categorized under reticle degradation by extensive use. That includes the high-volume manufacturing-oriented conditions of high source power needed to obtain competitive throughput. For each aspect of EUV mask defectivity, and hence each type of defect, the paper reviews how the community tackles them and how their possible impact on the result of wafer printing with a given EUV reticle is minimized. This includes a summary of the authors' own contribution to related learning and developments. Finally, a personal interpretation is given of what are the remaining open items before a workable or full solution can be considered in place.

Keywords: contamination; EUV lithography; mask defects; ML-defects; particles.

***Corresponding author: Rik Jonckheere,** STS-AP, imec, Kapeldreef 75, Leuven 3001, Belgium, e-mail: Rik.Jonckheere@imec.be

www.degruyter.com/aot
© 2017 THOSS Media and De Gruyter

1 Introduction

Extreme ultra-violet (EUV) lithography is in development and targeted for introduction into high-volume manufacturing (HVM) of integrated circuits from the N7 or N5 node onward, depending on company-specific interpretation and definition of these. The general understanding is that reliable source operation and resist resolution, sensitivity, and line-edge roughness (LER) met simultaneously are rated as the top two focus areas [1]. EUV masks (or reticles, used as synonym in the present context) cover the third and fourth place in this ranking, with as a description, respectively, keeping the mask defect-free, and mask yield and defect inspection/review infrastructure. Both of these aspects are covered in this article.

In earlier publications [2, 3] four main types of defects on a typical EUV mask were mentioned:
– Absorber pattern defects
– Particle contamination
– Local cap deterioration
– ML-defects.

In the present coverage of the topic of EUV mask defectivity, we actually make a somewhat different classification than just those four, as can be seen by the titles of the several sections below. The alternative way of discussing the aspects of defectivity reflects the process and sequence of learning, starting from the time that a first EUV lithography tool became available at imec.

For each aspect of EUV mask defectivity, a summary of the evolution to the state-of-the-art way of coping with it is now given. Subsequently, this article discusses how far this is a workable method or already a full-proof solution.

2 Particle contamination

At the time when the first full-field EUV exposure tool (ASML Alpha Demo Tool – ADT) was introduced in the field (2008), it was expected that wafer printing without impact of mask particles would need to be obtained by

ultra-clean handling of the reticles, fully avoiding such particles. This scenario was dictated by the knowledge of the difficulty of finding a material that would not be too absorbing at the EUV wavelength and could, therefore, be considered as a pellicle (see Section 7). At this time, one used the so-called storage boxes for reticles. They essentially were a part of the airlock system to bring a mask into the vacuum system of the EUV scanner for exposure. These were already using the concept of hard pellicle that is removed at the time of actual exposure. Transport of the reticle used the same shipping boxes as established for deep-UV reticles. Manual handling was used to transfer the ADT reticle into the storage box. Even when doing it in a highly clean environment, this appeared to be the dirtiest step [4].

2.1 Backside particles and evolution in mask handling

At this time, backside particles were still the major concern. Frontside particles did not yet get much attention (while they eventually become most critical). Backside particles were understood to lead to focus- and overlay-related errors. Upon fixing a reticle onto the electrostatic clamp on the reticle stage and its repeating scanning movement for exposing subsequent dies on the wafer, a particle on the backside of a reticle potentially causes a local non-flatness of the reticle [4], as illustrated in Figure 1A. The effective impact of a particle is a function of its mechanical properties (predominantly size and hardness). A pin-chuck type clamp is used, so that the reticle is only making physical contact at the pins. These have a relatively low coverage compared to the full area of a 6″ mask. Despite that, high-enough particles located between the pins of a given height can have such focus or overlay impact. In practice, such effects can be expected for particles of several microns high.

A more complicated situation emerges when such a critical backside particle, brought onto the clamp by the first reticle, subsequently stays on the clamp, while this first reticle is unloaded and therewith causes a hotspot in the corresponding position in the exposure field. This particle will cause similar reticle distortion (and hence overlay and focus troubles) for any subsequently loaded reticle. Recovering from this situation when still using ADT was disruptive, as it required venting the main chamber for physical cleaning of the reticle clamp. A major lesson learned was that, on future EUV scanners, more effort would be required to avoid, and even eliminate, critical particles on the reticle clamp. Already

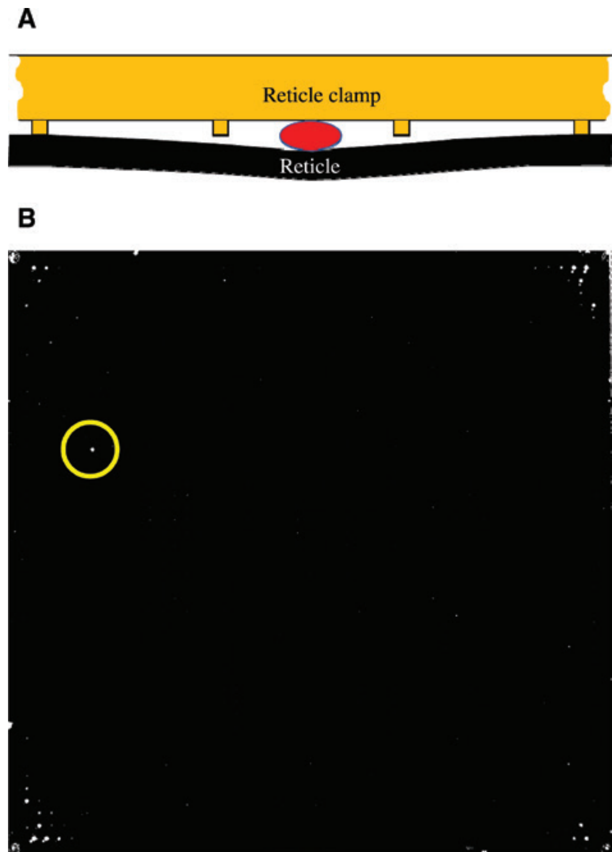

Figure 1: Illustration of the effect of backside particles: (A) Upon reticle clamping, a thick-enough particle can become squeezed but causes the reticle to distort. (B) Example outcome of a backside inspection. While artifacts are present on the corners and the edge of the mask [5], the intention is to avoid particles as the marked example, when these are expected to cause effects as illustrated in (A).

during ADT times, we started routine backside inspection to minimize the occurrence of such particles upon (manual) loading of a reticle into the reticle storage box. Inspection was visual and, therefore, not quantitative. Getting the backside of the reticle particle-free above a certain expected critical size (in view of overlay or focus control) has been the main drive to install an EUV mask cleaning capability in close vicinity to our ADT. Our cleaner accepted the reticle from the same carrier as the ADT itself, i.e. the above-mentioned storage box.

As we migrated to the so-called pre-production exposure tool (ASML NXE-3100) in 2011, we could benefit from the implementation of the so-called EUV pod, also known as the dual pod or pod-in-pod [5]. The outer part corresponds to the format and principle of a standard mechanical interface (SMIF) pod in use for mask transfer between tools inside a mask shop (a so-called RSP200). Putting the reticle within a second box (or pod) inside it

has the following purpose. The inner pod (called the EIP, short for EUV inner pod) consists of a base plate and a cover, typically made of metal for better compliance with the vacuum system of the EUV scanner. The base plate has the role of a removable hard pellicle, which protects the pattern side of the reticle at each moment in time inside the exposure tool, except when it is clamped onto the reticle stage, so that it can reflect the EUV light for wafer exposure.

In a first expansion of our cleaning tool, we assured compatibility with these EUV pods and reduced manual handling to a minimum: each reticle is assigned to a fixed EUV pod, in which it is placed by automated handling starting from an RSP200. Only for loading into the latter, from the shipping box, was manual transfer still used. In a later stage, it could become a target to receive each new reticle from the mask shop already in an EUV pod, but this is not yet common practice. To further improve our avoidance of critical backside particles, a backside inspection capability was subsequently built into our mask cleaner [4, 6]. At this moment in time, this gave us a unique, actually the world's first, infrastructure for integrated automated handling, backside inspection, and cleaning of EUV reticles. Mask cleaning is discussed in Section 3. This integrated infrastructure made it possible to routinely check reticles in use on the NXE3300 for critical backside particles by putting the reticle in its dedicated EUV pod onto the cleaning tool for backside inspection, using all-automated handling. If the inspection result was found in conflict with the set criterion, the reticle was cleaned and subsequently re-qualified for further use, all via automated handling.

What is the critical particle size to avoid any overlay or focus on a problem is a very relevant question. Basically, this relates to the height of the particle, together with its mechanical properties such as elasticity or hardness. The inspection capability inside our cleaner is based on the principle of dark-field inspection. This uses the intensity of scattered light as a quantitative output that may relate to the physical size of the particle. At first, a criterion set was based on evidence that such a particle caused a hotspot in a map of a printed overlay [7, 8]. On two occasions, we correlated the criterion to height-sensitive defect review on external tools [8], and our day-by-day way of working continued based on empirical interpretation of the intensity-based inspection result. Over time, we have refined the criterion based on residual evidence that particles with detection intensity below the assumed threshold were still migrating from one reticle to another via the reticle clamp.

Figure 1B shows a representative example of a reticle backside inspection image. While artifacts occur, especially near the corners and edge of the mask, these have been shown to be non-critical in view of their limited height [8]. The way of working focuses on avoiding that real particles, like the one marked, can migrate to the reticle clamp and from there onto further reticles. As a quality area, a centered square of 146-mm side is used, which includes the total area where the electrostatic clamp has pins, and which clearly exceeds the area corresponding to the field on the frontside of the reticle.

Another weakness of this working mode is that the backside particle monitoring of EUV reticles in use on the NXE3100 was based on sampling. Hence, it still could not be totally avoided that a reticle with an unacceptable backside particle (according to the criterion used) got onto the reticle clamp anyway. Yet, such events were already clearly much rarer than on ADT. As shown in Figure 2, it has been possible to reduce occurrences of overlay hotspots both in frequency and residual overlay impact [8].

With the advent of the NXE3300 in 2015, the next step became possible: means came in place to physically avoid that reticles with unacceptable particles on their backside could be loaded onto the reticle clamp. The ASML NXE3300 at imec is *in situ* equipped reticle backside inspection (called RBI), using a similar principle but using another wavelength. In practice, we have obtained good correlation between the backside inspection in the cleaner and the RBI module *in situ* to the NXE3300, as shown in Figure 3. Note that RBI is also not height sensitive. The next major step has been that mask backside inspection is no longer based on sampling: all reticles entering the scanner are inspected. In case a reticle does not meet the

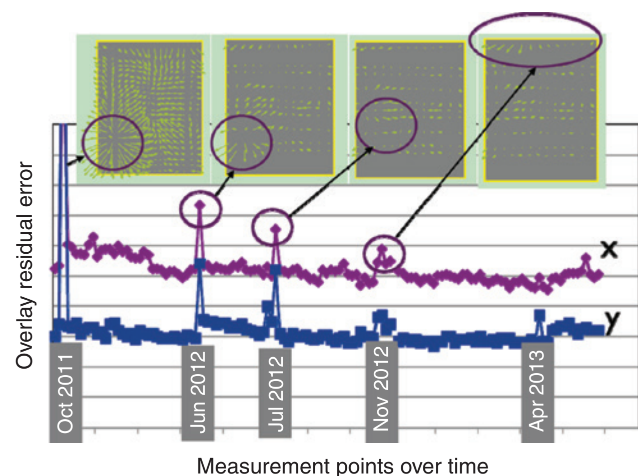

Figure 2: Over time reduced occurrence of elevated printed overlay errors for NXE3100 (shown as intra-field residuals), correlated to reduced occurrence of critical particles on reticle backside during exposure (adopted from Ref. [5]). The small overlay maps on the top part of the figure include hotspots correlated to the position of the particles on the reticle backside.

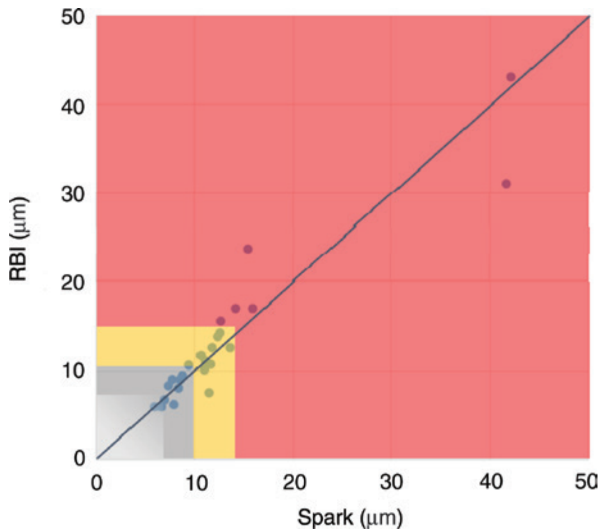

Figure 3: Correlation result for the backside inspection inside the cleaner (SPARK) and inside the NXE3300 (RBI). Both tools use darkfield imaging and scattered light intensity to give an estimate of physical size.

set criterion, it can be automatically prevented from being loaded onto the reticle clamp for exposing wafers. We have empirically installed a detection threshold that is a good compromise between evidence that a detected particle still moves onto another reticle via the reticle clamp, on the one hand, and a too frequent need for cleaning because of a reject by the scanner, on the other hand.

What are the potential ways to improve this further? While we have been able to establish a good correlation between both backside inspection capabilities, none of them physically measures height. We continued with a criterion based on scattered light intensity. In principle, one could benefit from having a height-sensitive review tool in close vicinity to the EUV scanner, so that upon exceeding a certain detected size during backside inspection, a physical height measurement can be made to decide whether a defect is critical or not. Second, trying to make a generic correlation model between detected size and obtained local overlay or focus error would be beneficial. Yet, this requires dedicated characterization experiments and, anyway, would suffer from limited prediction capability because of the different impact of a particle depending on the material it consists of. Depending on its mechanical properties such as hardness or elasticity, the height of a particle will translate into a physical height as clamped and, therefore, an amount of local deformation of the reticle.

Throughout the reasoning above, the harm of particles is estimated for the case where their height exceeds the height of the clamp pins. Because of the low density of the pins, the probability that a particle lands on top of a pin was, thus far, neglected. In principle, the probability for a particle on top of a pin is not integer zero. In such rare cases, its height can be expected to become critical from smaller values onward, again depending on the material properties of the particle.

Totally excluding backside particles from occurring is a challenge: while the pod-in-pod principle protects the backside of the reticle by putting a first protecting box into a second one is, in the first place, at each point in time, still dependent on the cleanliness of the EUV pods in use. This calls for having a capability in place to frequently inspect and clean them. Third, inside our cleaner and inside the EUV scanner, the particle-free state depends on ultra-clean handling that fully eliminates the probability of adding a (potentially) critical particle on the reticle backside. Our backside inspection implemented in the NXE3300 is also applied to monitor for the latter risk: beyond the reticle entry into the scanner, backside inspection is also executed for every reticle upon unloading it from the reticle clamp, i.e. after completion of the exposure batch, before the next reticle is loaded onto the reticle stage.

2.2 Pioneer position for evaluation of frontside particles

The above-described infrastructure, based on automated handling and use of dedicated EUV pods, has also allowed us to investigate how clean the pattern side of a reticle remains in the EUV scanner during its use for exposure. At all times, this side is protected by the base plate of the EIP (within practical limits), except when the reticle is clamped on the reticle stage, typically at the time of exposure. Production use of this way-of-working requires a zero chance that a critical particle (i.e. one that would cause a printing defect) can contaminate the pattern side of the mask during the time that it is unprotected. A few years back, we have been one of the earliest parties to demonstrate that this was not the case for the earlier NXE3100 [7]. The evidence even showed that during the exposure of a wafer, a particle got on the mask pattern. It caused a printing defect from a specific die on the wafer onward, and it was repeating on all subsequently exposed dies and wafers. Such particle adders on the reticle can be detected using wafer inspection followed by repeater analysis. The technique is illustrated in Figure 4. Today, it is routinely used to find evidence of particle adders after a certain time of using a reticle: wafer printing freezes the state of the reticle at the specific point in time, for example, exposed immediately after loading

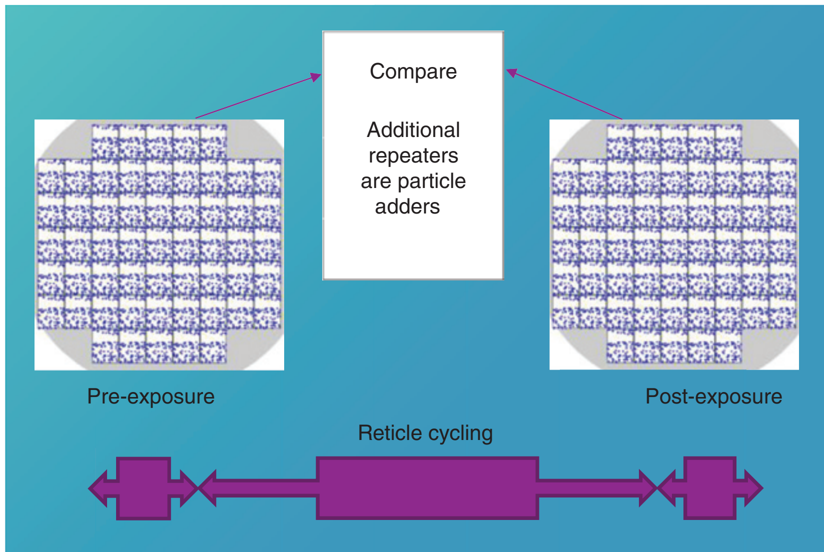

Figure 4: Schematic representation of the technique of combined wafer inspection and repeater analysis to find evidence for added particles on the pattern side of the reticle, while it is continuously on the reticle clamp for exposure. Such a particle is detected as an additional repeating defect on a newly exposed wafer compared to an earlier wafer.

the reticle into the scanner. Any additional repeater found on a wafer that was exposed later than such a reference wafer (while the reticle is at all times on the reticle stage) proves that the particle was added to the reticle inside the scanner. ASML has made utmost endeavor to minimize the chance of such frontside particle adders to one adder in 10 000 reticle loads and targets for further improvement [9]. The difficulty to demonstrate such capability without really elaborate and lengthy experiments initiates a call of the industry for a genuine pellicle solution. In practice, for NXE systems in the field run under production conditions, typically higher frontside particle adder rates are reported, exceeding such ASML data [10, 11]. Despite the difficulty of finding an appropriate material that can serve as an EUV pellicle, in view of the typically always too high absorption of EUV light by any material, its availability is considered essential by multiple IC manufacturers. Except for some memory manufacturers, the answer clearly is that the particle adder rate should be zero, by strong preference.

Whereas the higher particle adder rate is today typically characterized using optical wafer inspection, that may not have enough sensitivity to detect all particle sizes that matter. Moreover, it is not (yet) applicable to typical mask layouts (see below). Special test reticles with equal lines and spaces that cover the whole exposure field are typically used [12], with a half-pitch that is representative for the intended technology node, i.e. typically now 16 nm or 22 nm. For this dedicated pattern, the chance that a fall-on particle will cause a printing defect, and therefore that it can be detected, is (more or less) maximized. Optical wafer inspection typically uses comparison of several dies on a wafer, a principle close to 'die-to-die' inspection. Optical wafer inspection is typically not resolving the pattern itself. Detection is based on a deviating gray level from the uniform background. It is very capable to detect (quasi-)bridges between two adjacent lines, but these correspond to particle sizes in the order of 70 nm on the mask. Yet the critical particle size on the mask is close to the intended half-pitch on the wafer, per a long-lasting rule of thumb in 4× lithography. Already a particle of such size could cause a 10% increase in the printed CD on wafer, i.e. the definition of a (printing) defect. However, it is typically not detected by optical wafer inspection, even when increasing its sensitivity, as by inspection of an etched stack instead of the resist image [13]. For fall-on particles in the range ~20–70 nm, today, one would need to rely on other wafer inspection means, such as using an electron beam (e-beam) [14]. Despite having the required resolution, it is less attractive because of longer inspection times. Multi-beam inspection has the capability to overcome this in the future.

Patterned mask inspection (PMI), further discussed in Section 5, historically has a better sensitivity to detect particles on a reticle because it has the strong advantage of inspecting the four times larger pattern on the 4× reticle. It can be expected to cover the range of ~20–70 nm particle size on the reticle, where optical wafer inspection lacks sensitivity. Yet, particle adder qualification via PMI misses the capability to indisputably demonstrate that a particle

was added to the reticle in the EUV scanner, rather than in the inspection tool, itself. In this case, there is no 'freezing' of the status of the reticle possible in the same way as when using wafer inspection. For PMI, the reticle must be unloaded from the scanner, and while being transported and handled via the dedicated EUV pod, it is yet unloaded inside the inspection tool and at this time unprotected for the time of effective inspection, and possibly during handling of the reticle inside the inspection tool. While such a mask inspection tool can be demonstrated to have very low particle adder rate, its specification is likely not (integer) zero either. This is the problem of the issue of particle adders on the pattern side of an EUV reticle (without a pellicle). It is a quest for relatively very rare events, and when an adder is detected, then what was its cause? Wafer-based inspection does not have this disadvantage and can indisputably prove that a particle was added on the reticle inside the EUV scanner.

However, compared to PMI as means to find particle adders on the pattern side of a reticle, the wafer inspection approach has another important disadvantage. As was said before, optical wafer inspection does typically not resolve the mask pattern. The pattern density of a typical layer of an integrated circuit design is not as uniform as in a dedicated line-and-space test layout. Particles that fall into less dense areas of the layout, or that become an isolated defect in a clear area, have a much smaller printability and are, therefore, only detected during wafer inspection from an even larger size than the above-mentioned ~70 nm. While one can still use a principle of die-to-die for wafer inspection, added particles of a same size would be missed in (more) isolated parts of the design. The use of die-to-database in combination with higher resolution wafer inspection (such as based on e-beam [15]) can help. However, if a fall-on particle does not print, because, for example, it is located on a large opaque pattern feature on the mask, then based inspection will, of course, always miss it. Moreover, at a later point in time, the particle may move and become printable. An option to monitor for added particles may be to routinely inspect exposed production wafers on a sampling basis, using a best-suited wafer inspection, but this adds to the lithography cost.

3 Evolution of EUV reticle cleaning

Backside particles, as described in Subsection 2.1, have historically been the prime need for a mask cleaning capability at the wafer fab, in close vicinity to the EUV scanner. Whereas, in principle, this could have been addressed by a 'backside-only' clean capability, in practice, this was originally not realized on our cleaner. The pattern side of the reticle is, in the case of using liquid media, also wetted while cleaning the backside. Over time, we have optimized a backside dedicated, frontside minimized clean. Additional goals of mask cleaning can be to remove frontside particles (as discussed in Subsection 2.2) and frontside contamination by carbon growth or something similar (see Section 4). In the original expectation that a fixed pellicle solution would not be available for EUV reticles, the requirement was that a reticle would need to survive in the order of 100 cleans during the time it is in use.

On our mask cleaning tool, historically, a choice has been made for dilute aqueous media [16–18]. Other teams have reconsidered cleaning based on a mixture of sulfuric acid and hydrogen peroxide for EUV reticles [19], whereas in the past, such SPM-based cleaning was banned for deep-UV reticles because it was deemed responsible for haze formation. While evolving from early results where even just four cleans were already causing a modified printing performance of a reticle [4], we have demonstrated that the printing performance of a reticle could be kept stable up to 100 repeats of our cleaning process [20]. Likely at the microscopic scale, one could still find evidence of the impact to the ruthenium-capped ML by repeated cleaning. A study based on surface chemistry is expected to be valuable. Also, a study of the interaction with events occurring during storage of a reticle remains relevant. Cleaning also impacts other process steps such as repair (discussed in Section 8). We have experienced an increased difficulty to make absorber etch in the repair tool stop properly on the capping layer, which is assumed to be due to residual impact by cleaning. Our experience supports the description in Refs. [21], [22] that the upper silicon layer underneath the Ru cap becomes oxidized, which can lead to volume expansion and subsequent cracking of the Ru cap.

Such residual impact of repeated cleaning is also expected apparent at the unprotected sidewall of an etched-ML black border [20]. The latter is not explicitly discussed in this review. It is the industry's present solution to deal with the fact that the image border around the pattern on the reticle is not sufficiently dark, causing CD impact in the outer part of adjacent dies, unless the die separation on the wafer is taken larger than is typical in semiconductor manufacturing practices based on deep-UV. Possible specific defects of such etched-ML black borders have been assessed in Ref. [23]. Whereas ML roughness can become worse over time because of impact by repeated cleaning of the mask [4], it is also a point of attention for blank manufacturing. From some dedicated studies [24, 25] the high-level learning is that ML roughness will cause reduced reflectivity of the ML, leading to a

loss of achievable image contrast relative to the absorber. In similar ways, it can, at the cost of inspection sensitivity during blank inspection (see Section 9), as it requires an elevated threshold to minimize the background noise and false detection rate [26].

4 Outlook to EUV mask degradation effects

Several publications have studied carbon growth and oxidation effects as potential deterioration effects for EUV reticles [27–29]. The basics is that hydrocarbons and water vapor, when present in the vacuum system, can adsorb at the surface of the mask and at this time be dissociated such that, respectively, a graphitic film can grow on the surface, or the resulting reactive oxygen can oxidize, for example, the capping layer. In the case of an Ru cap, it is understood that the reactive oxygen may predominantly oxidize carbon contamination that has grown on top of the Ru cap and, make it volatile, which is referred to as the self-cleaning property of Ru-capped ML [30]. If the partial pressure of hydrocarbons or water vapor is inappropriate, carbon growth and/or oxidation effects can be very pronounced. For the ADT system, for example, carbon growth was reported [31]. For our NXE3100 reticles, we have not seen (true) evidence that such contamination growth occurs, yet with one exception left aside. During a cleaning experiment (using an earlier process than the established one, as discussed under Section 3) with a routinely exposed reticle, one clean appeared to have decreased the printed dark CD, whereas it remained stable subsequently for the next more than 10 cleans [4]. A possible explanation is an increase in reflectivity through the removal of EUV-induced carbon growth and/or removal of conformal carbon growth onto the dark feature on the mask.

Because EUV scanners, so far, have had lower source power than needed for HVM-typical throughput, a key question is how such deterioration effects will evolve on future scanners. It is considered a possibility that even additional effects such as multilayer compaction or Mo/Si interdiffusion will start to contribute to the deterioration of the capped multilayer. A major difference between an EUV reticle and a mirror of the optics remains that a reticle routinely leaves the vacuum environment. To investigate such possible additional deterioration effects ahead in time, yet in representative conditions for future EUV scanners, TNO has built the ‘EBL-2’ facility [32], and dedicated contamination assessment experiments are in preparation.

5 PMI

In the first place, PMI for EUV reticles has the same role as for deep-UV reticles: detect absorber-type defects. These consist of a local surplus absorber or missing absorber, also known as opaque and clear defects, respectively. Such ‘hard’ defects are typically caused by particles that locally obstruct and influence (exposure and) development of the image in the resist and/or its transfer to the absorber layer during etching. Typically, inspection tools have a sensitivity that surpasses the need based on printability of such absorber defects. State-of-the-art PMI tools can typically also detect add-on particles, as discussed in Subsection 2.2. Historically, the wavelength used for mask inspection has lagged, compared to the wavelength used for lithography. The main driver for the inspection tool is to meet both resolution and throughput requirements, without going into unnecessary costs of redundant complexity and possible overkill. The inspection tool family of at least one vendor [33] has, for such reasons, only started to use a wavelength of 193 nm at a time that 193 nm lithography went into the immersion era, and quickly evolved into double patterning. Before that, a 257 nm wavelength continued to be used for a long time after 193 nm was initiated as the leading lithography wavelength. Another vendor has historically chosen to make the inspection optics better reflect illumination conditions of the lithography tool, in addition to the wavelength [34, 35]. In deep-UV lithography the state-of-the-art PMI tools based on 193 nm wavelength have had as a main purpose to assure that (i) all absorber defects are found, such that they can be repaired (see Section 8), and (ii) it can be assured based on through-pellicle inspection that there are no particles underneath the pellicle that can be expected to print (see Section 7). For both purposes, at-wavelength review (also called actinic, see Section 6), intentionally using the same wavelength and illumination conditions as for exposure, is subsequently used to confirm accurate repair or, as a minimum, assess sub-threshold printability effects of residual ‘defects’ (Note the hyphenation because a ‘defect’ is to be considered a defect if it causes at least 10% influence to the printed size of a feature of the pattern in its neighborhood, unless the defect, itself prints as a standalone unwanted feature).

E-beam inspection has been proposed as an alternative to 193 nm-based PMI with better resolution (see, for example, Ref. [36]). While, historically, ample resolution is typical to e-beam-based imaging, throughput limitations make it less obvious to establish it as the standard inspection technique. Anyhow, initiatives to make it much faster such as by multiple beam [37] or by using it in combination with projection optics [38] are underway. Subsequent

to e-beam-based inspection, actinic defect review, as described above, remains key to decide correctly about repairs or residual effects, based on estimated printability. The second task of inspection, i.e. through-pellicle inspection, is clearly not supported by e-beam-based inspection.

Now, discussing EUV reticles, the above-mentioned 193 nm based inspection tools are what we have at our disposal. Also, e-beam inspection can help if resolution becomes the driver. For at-wavelength (=actinic) EUV-based inspection, there appears no commercial, standalone tool on the horizon yet [39]. For the first task (item i above) of the PMI, one probably does not (yet) need the resolution of EUV-based inspection, and one may avoid the tool complexity and cost. Yet, as regards the second task (ii above), i.e. through-pellicle inspection, either a 193 nm transparent EUV pellicle will be needed, or an actinic EUV-PMI tool becomes unavoidable. The discussion in Subsection 2.2 about particle adders on the pattern side of a reticle may be the loudest call for EUV-based inspection. One should interpret, in the author's opinion, putting actinic PMI as a missing item in an estimation of the EUV mask infrastructure readiness [10] in this way.

On a more experimental level, other endeavors toward EUV-based PMI are underway (as an example, see Ref. [40]).

6 Mask review to confirm the mask 'through scanner spectacles'

Historically, an a aerial image metrology system (AIMS, also a trade mark of Zeiss) has been the established tool of preference in both KrF and ArF lithography, for printability assessment of detected defects and/or of confirmation of their mitigation such as by repair. Such capability is historically considered a key component in the overall tool set of a mask shop. Because of its complexity and to assure a proper return on investment, such an AIMS tool based on EUV has required a strong joint investment program and a long development time. Sematech has initiated and monitored the so-called EMI consortium to assure that such a tool became available to the contributing stakeholders and to subsequently establish such possibility for other interested parties. As a very positive evolution in the fall of 2016, the first shipment to the field was announced [41, 42]. With this, defect printability studies at EUV wavelength, as well as repair attempts for the ML-defects discussed further in Section 9, no longer need to be executed by wafer printing as is the common practice so far, enabling a faster turnaround, as required for production.

A similar capability, yet not as a standalone tool, has been in place already longer at LBNL with SHARP [43] and its lower NA predecessor AIT [44], as part of the CXRO synchrotron beamline. A similar experimental capability has been described in Refs. [45, 46].

7 What will change with the advent of EUV pellicles?

An EUV pellicle solution is under development by ASML [47–49] and other stakeholders [50], including imec [51–54]. While a pellicle is intended to overcome the issue of particle adders on the pattern side of a reticle (Subsection 2.2), every aspect discussed in this article thus far (Sections 2–6), is affected in some way. EUV pods that are compatible with a pelliclized EUV reticle are meanwhile available [55]. Equally, it was demonstrated that these are appropriate for overseas transport of a pelliclized reticle in the present format. ASML's solution is based on the principle of a removable frame that is held in place by dedicated studs glued onto the reticle, on which it clips. In common practice for a deep-UV mask, the frame is glued to the reticle. Only a hermetic solution can fully avoid that a residual risk for particles exists. Atmospheric pressure variation is, in case of a deep-UV pellicle, overcome by means of vent holes on which a particle filter is applied. This sufficiently excludes the chance of a particle entering the pellicle 'cavity'. In the case of EUV, such a frame with just one or a few filter-protected ventilation holes is not compatible with the pumping – and venting rates required by the vacuum system of an EUV scanner. The proposed clip-on frame to cope with these rates [56] uses a micro-gap between the reticle and the frame. Such gap has a higher risk that particle adders are not fully avoided, despite such expectation of a pellicle by the users, as discussed in Subsection 2.2.

The integrated infrastructure for automated handling, backside inspection, and cleaning described in Subsection 2.1 must become compatible with a pelliclized reticle. Meanwhile, the capability to load a reticle into a dedicated EUV pod for a pelliclized reticle by automated handling, together with its qualification of required backside cleanliness for use on the EUV scanner, was demonstrated [57]. For mask cleaning, the target no longer is to be able to clean a reticle as many as 100 times during its life without a change in printing performance, as it was originally targeted on the assumption that EUV would need to work without pellicle [58]. As a particle-free backside is now the main driver for routine cleaning, the capability of a backside-only clean without impact to the pellicle in place on the pattern side

is essential. If the frontside needs cleaning, this means, in case of the present ASML frame [48], that it is taken off this at this time. A frontside clean with the studs still in place is required, unless it shows practically that they are removed beforehand, and placed back afterward.

Inspection for particles on the reticle frontside, as previously discussed in Subsection 2.2, for the case without pellicles, can be continued in similar ways when a pellicle is in place. Analysis based on wafer printing and – inspection could identify if there is a particle added to the pattern. Possibilities for such adders in the pelliclized case may include (i) particles that were present underneath the pellicle already and that subsequently moved into an area that prints (more), (ii) additional particles due to limited airtightness and, therefore, non-zero risk for entry of new particles, and (iii) big particles that land on the membrane and are not sufficiently out of focus. In view of the membrane stand-off distance from the pattern side of the reticle of 2.5 mm [56], the expectation is that particle sizes from a couple of micron onward on top of the membrane can still cause a defective area of the wafer print. While it is not sure if wafer inspection could detect this, the existing infrastructure for particle inspection on a pellicle, as used on a deep-UV reticle, is confirmed as being capable for EUV pellicles [59]. Removal of such a particle from the pellicle membrane might be extremely challenging in view of the typically very vulnerable structure of an EUV pellicle membrane. Replacing the pellicle may be an easier solution than cleaning off such particle from its surface. However, replacing the pellicle brings new risks for particles on the pattern plane and, hence, additional inspection is needed. Through-pellicle inspection of the pattern plane requires that it can be done at the EUV wavelength (see Section 5), unless the pellicle has sufficient transmission at the wavelength of optical inspection [60]. Unless one of both options becomes a reality, wafer inspection may be the only possibility with the pellicle in place. However, it is known to lack sensitivity down to the critical particle size (see Subsection 2.2). Last, actinic defect review on mask (see Section 6), also to check for printability of particles found, can be assumed pellicle capable, as it is actinic.

8 Repair of absorber defects and more

Absorber defects are not at all EUV specific and were therefore not discussed at length in this article (see Refs. [2, 61]). Absorber defects are mostly caused by resist process-induced defects or defects in the absorber layer on the blank. Also, on EUV reticles, surplus – and missing absorber defects are repaired by, respectively, local removal and deposition, called opaque and clear repair. Today, e-beam and probe-based repair techniques are most common for EUV reticles [62, 63]. In the case of an EUV reticle, repair also imposes special care onto mask cleaning (as discussed in Section 3). If the capping layer is pre-affected by the cleaning process, the opaque repair process may fail because Ru has lost its ability as an etch-stop layer.

For EUV reticles, there is another type of defect that can be overcome by extending the functionality of the absorber defect repair. This relates to the ML-defects, discussed in Section 9.

9 ML-defects: the other mask defectivity challenge for EUV lithography

The previous sections covered both the wavelength-independent absorber defects, and the somewhat more pronounced EUV-typical effects of particles and other contamination effects. The challenge of the most EUV-specific defects remains to be faced and solved. ML-defects relate to the reflective mirror of the mask, formed by a Mo/Si-based quarter wave stack, similar to the mirror elements of the projection – and illuminator optics of the EUV scanner.

This type of defect on an EUV mask is the one that the author estimates as having had the largest contribution to the related learning by the EUV community and its path to an industry-accepted solution. Apart from the particle issue discussed in Section 2, it has historically been a potential showstopper for EUV lithography. Also, here, solutions are underway. This topic is now discussed in a number of sequential steps, covering characteristics and potential solutions, including limitations of the latter.

9.1 ML-defects: what they are?

ML-defects are defects of the ML mirror that makes the EUV reticle reflective, in the same way as the mirrors in the optics of the EUV scanner. In the latter, they do not matter (as much) because one does not image the plane of the mirror, unlike the mask itself.

On the mask, such localized defects print, in the first approach, from the same (lateral) size onward as absorber defects. However, what is critical is that they typically are only just one or a few nanometers high or deep bumps or pits, respectively [64]. In view of the principle of the ML as a quarter wave stack with an 7 nm period, the position of the defect has a deviating phase compared to the surrounding area on the mask. For this reason, these defects are also often dubbed as phase defects, but essentially, there is also a local re-distribution of the intensity involved (=amplitude aspect). The phase nature can lead to pronounced through-focus printing behavior [65] or, in different words, to a tilt of the Bossung curve for an equal line and space pattern [66, 67].

ML pits are typically rather artifacts of polishing of the LTEM substrate, whereas bumps can originate from particles added during the ML deposition process or already on the substrate.

9.2 Direct ways to address ML-defects

Historical work has attempted to find solutions to directly 'repair' such defects. This included techniques to induce local compaction of the ML to overcome bump-type defects [68], but as such it did not evolve into a good solution.

Essentially, the preferred solution for ML-defects is not to have such defects at all and to assure that the commercial blank quality is fully defect-free. At this time, this is not yet the case, although some publications report reaching champion plates that do (e.g. [69]). The achievable yield for such blanks is as yet still limited. Meanwhile, the industry has started to look into possibilities to 'live with' a limited, say single-digit, number of such defects on a blank. As discussed further in Subsections 9.4 and 9.6, such situations may be manageable in a production environment, as there are ways to compensate or avoid the printing impact of a small number of such defects.

The MBDC, a former initiative of Sematech – the Mask Blank Development Center, has focused on ways to reduce the number of such blank defects year after year, among others, by optimization of the deposition tool [70]. Also, the printability of defects was investigated, as well as metrology by transmission electron microscope technique [71], and ways to induce smoothing [72]. The latter technique optimizes the deposition condition of the subsequent bilayers of the ML mirror such that the height (positive for a bump and negative for a pit) and width of a defect inside, or underneath, the ML is smoothed out toward the surface of the ML, such that the local distortion in the upper layers of the ML is reduced in height and possibly laterally smeared out. Whereas a model for smoothing has been published [73], at this time, each blank vendor considers the amount of – and the deposition recipe for – smoothing, a trade secret. As will be discussed in Subsections 9.4 and 9.6, this induces a complication when trying to mitigate their printing impact of ML-defects. At this time, it is also important to realize that assuring that a ML-defect fully flattened at the ML surface is, in principle, not satisfactory to make it non-printing. It is very true that the printability defect does very much depend on how the height and lateral size propagate through the ML as deposition proceeds from the first bilayers up to the surface of the full thickness ML [2]. While no one has published such experimental example, zero height ML-defects, with height taken here as merely referring to what it is at the ML surface, should not be overlooked and, with smoothing in use, can logically exist.

9.3 How to assure finding all ML-defects that matter

Blank inspection to find these EUV-specific ML-defects has historically (tried to) use existing optical tools that were originally intended for particle inspection on blanks or substrates, i.e. before or after coating the ML and other layers [74, 75]. This also explains, why historically, the capability of finding ML-defects with such tools was expressed as sphere equivalent diameter (SEVD). While the average, but not necessarily typical, morphology of a particle is a sphere, obviously SEVD, as a one-dimensional qualifier for a particle, can be understood to work well. For ML-defects, either bumps or pits of just a single-digit number of nanometers, it is obvious that the lateral size becomes relatively too dominating when attempting to correlate SEVD and printability. Additionally, an optical PMI has been further developed based on phase contrast to have good inspection capability for EUV blanks [76]. It is understood as essential that dedicated blank inspection needs to be capable of detecting all such ML-defects on the blank that could print on wafer, with a comfortable signal-to-noise ratio, so as to exclude an unacceptably high rate of false detections. Three generations of optical blank inspection tools, each using a certain wavelength [20], are considered to potentially be too surface sensitive (as illustrated in Figure 5). Related to the first requirement, i.e. to detect all such defects that could print, it has been demonstrated by others [77] and by us [65, 78–81] that the optical blank inspection techniques overlooked some ML-defects on a blank that were yet experimentally demonstrated of that nature, clearly printing, and found via inspection of

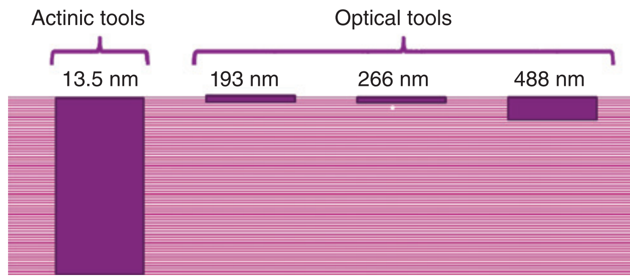

Figure 5: Overview of EUV blank inspection equipment, as reported in literature (adopted from Ref. [20]). The entrance depth into the ML, for the wavelength used, is just for illustration.

through-focus exposed wafers followed by repeater analysis, i.e. the same technique as described in Subsection 2.2. An example of such a defect that was first found on a wafer, and overlooked by blank inspection, is shown in Figure 6. An example of the second requirement, i.e. low false detection rate, is discussed in Ref. [79]. A good correlation between blank inspection and printability performance is clearly essential.

Actinic blank inspection (ABI) has been under development in Japan through EIDEC and its predecessors Selete and MIRAI [82–85]. In recent collaborative work between EIDEC and imec, such good correlation between the inspection signal intensity and printability on ASML's NXE3300 installed at imec was demonstrated for the HVM-oriented ABI tool under further development [86–89]. ABI blank inspection was found to capture all printing ML-defects down to hp 16 nm. As shown in Figure 7 a threshold for printability, yet dependent on pattern half-pitch, could be identified based on ABI intensity, above which a defect prints or not, depending on its relative position to the (lines and spaces) pattern. Using the ABI tool in high-magnification review mode [83, 84], similar to what was described in Section 6, proved very useful for this [89]. ABI is today's best capable blank inspection tool. This is not unexpected, because, as it uses the same wavelength as the scanner, it takes into account that the disruption of the ML throughout the ML contributes to the printing impact. Optical blank inspection techniques can be considered too surface sensitive [90]. A blank with single-digit number of ML-defects, or even zero, if that was qualified by ABI inspection, has maximum credibility. ABI inspection has become a tool of choice in demonstrating low numbers of blank defects [69]. A blank defectivity map obtained on this tool is a good basis for further mitigation work, as discussed in the next subsections. However, ABI has some limitations. A first one is that it can only inspect the ML blank, and not the stage before (i.e. mask substrate), nor

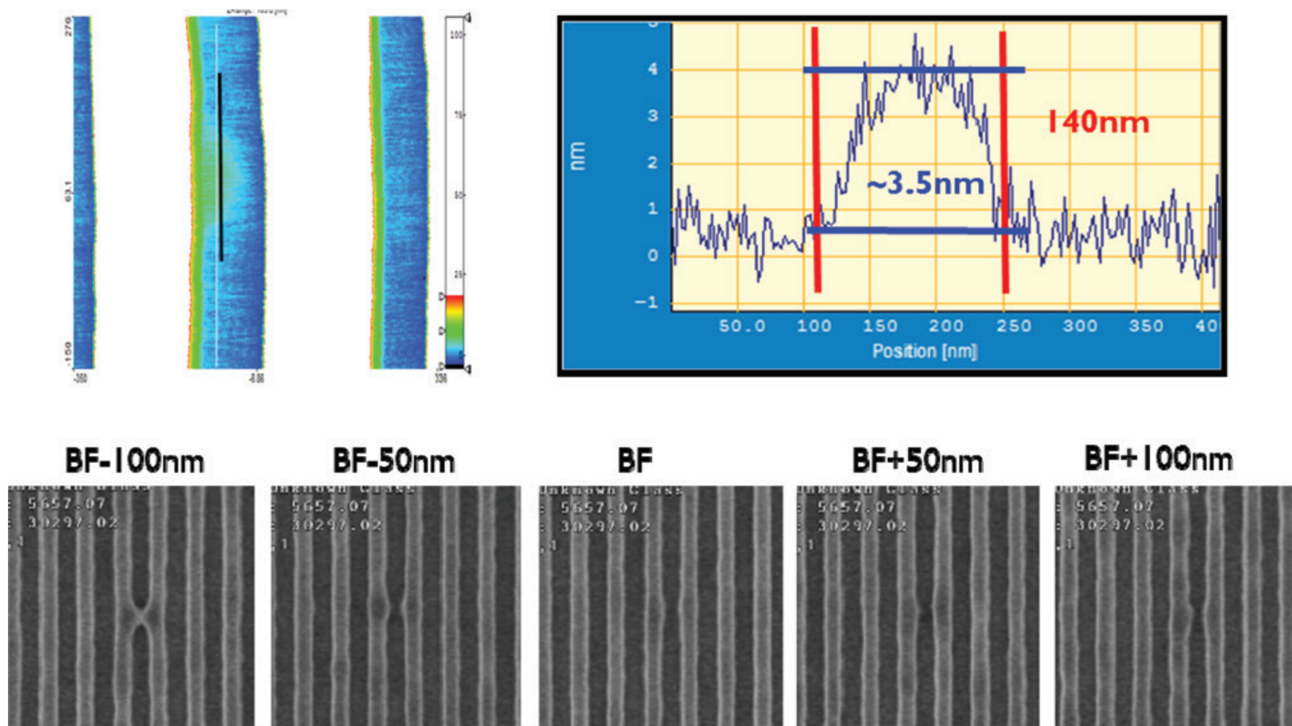

Figure 6: Detailed analysis of a printing bump-type ML-defect that was missed during optical blank inspection (example adopted from Ref. [65]). Top left: the top view as obtained by AFM; top right: cross-sectional view in parallel direction to the lines as shown, giving indications for height and width. Bottom row: asymmetric through-focus printing behavior on ADT, with BF as best focus.

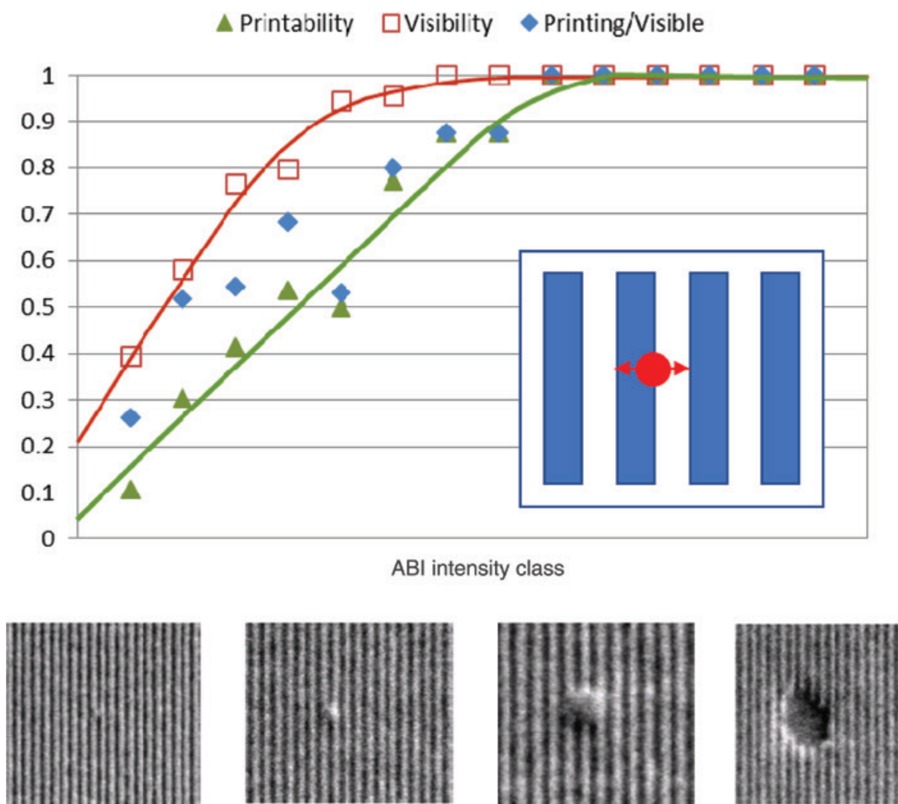

Figure 7: Correlation obtained between detection signal during ABI inspection (horizontal axis) and printability on NXE3300 (shown in green relative to vertical axis), for an equal line and space pattern (graph adopted from Ref. [89]). Detections with high ABI intensity all print (right). Intermediate detections partly print, which could be understood by the 50% chance of coverage of a defect (see inset, red dot) by an absorber line (shown in blue). Visibility on the mask by the ABI tool in mask review mode (shown in red equally relative to the vertical axis), is typically higher than printability (as shown by their ratio in blue). ABI mask review has allowed to determine the position of the defect relatively to this pattern (illustrated by the inset). The wafer SEM pictures below the graph illustrate the printing impact. Defects with large ABI intensity (right part of the graph and right-most picture) cause bridging between multiple pitches. At decreasing ABI intensity, these evolve over single bridges (second picture from left), to small printing impact (most left picture, printing as protrusion). Whether a defect of a given ABI intensity prints or not is determined by its portion residing inside a clear space between two absorber lines.

after (i.e. absorber coated blank). Another is that ABI, by concept, has lower sensitivity to detect particles (on an ML blank) [91]. This may mean that additional inspection on a particle-oriented blank inspection tool is appropriate to assure proper detection of particles during the blank fabrication process (from the substrate onward) and is essential to confirm absorber blank cleanliness at the start of the mask-making process.

At this time, it is also correct to state that the number of absorber defects on a typical blank still requires further improvement. Yet, these are already fully repairable on the final reticle (neglecting exceptional occurrences that indisputably exist). ML-defects, on the other hand, need to be further mitigated, preferably during blank manufacturing and the early stages of mask making, to minimize their printing impact (see Subsection 9.4). An essential pre-requisite for this has been the capability to detect them all, while the reticle is still in the ML-blank stage. Such capability is shown in place with the ABI tool, but, as it will be discussed in Subsection 9.5, also detailed knowledge of the accurate position of the defects becomes essential. This can be obtained using the high-magnification review capability of the ABI tool [83, 84].

9.4 ML-defect mitigation by hiding them

As a daily life analogy, let us consider dirt on the floor. We can sweep it under the carpet, as a quick solution. No, we need a better analogy because one can solve dirt by cleaning. A ML-defect is not dirt on the surface, it is rather embedded. So, let us rather consider it as a defect in a tile of our floor. We can replace the tile, or we can cover the defective tile by the carpet, such that it is not visible anymore. The floor corresponds to our mask blank; the carpet represents the absorber pattern. If a ML-defect ends up (fully)

underneath a dark feature of the absorber pattern, it is no longer printable. Equally, if such a defect is situated in an uncritical clear area of the pattern, it might also be tolerated. The latter includes two possibilities: (i) The defect is situated in a large clear area, where there are no features in the neighborhood that can be impacted by the presence of the ML-defect, and the ML-defect, itself, is still too small to print as an unintended dark feature. (ii) The defect prints, but it sits in an uncritical part of the mask pattern that does not contribute to the electrical functioning and performance of the obtained integrated circuit. Among the latter, we count dummy features that help to reach a better uniformity of pattern density across the considered design layer.

The challenging target becomes, 'Can all blank defects be assured ending up underneath an absorber or in uncritical clear areas of the design?' For a given intended mask pattern, one needs to find a blank that has no defects overlapping with the critical clear areas. The more blank defects present, the smaller the chance that such blanks can be found among the available ones in the EUV blank stock of the mask shop. Actually, one can help a bit with this 'pairing' action for a mask pattern and a suitable blank. Within the allowed centrality, i.e. placement error of the mask pattern relatively to the center of the physical mask blank, one can intentionally apply a small translation and even a small angle rotation of the pattern to cover more blank defects in this way. This is what is understood under the technique of pattern shift [92–94]. Yet it requires accurate knowledge of the defect on the blank, as will be discussed in Subsection 9.5. In addition, one of the four possible orientations of a mask blank may be preferred because more defects are covered by the intended pattern in this orientation. If the mask pattern consists of multiple dies, one can also tune their individual placement, such that a defect may fall underneath the border between dies (which is called floor planning [93, 95]). Dedicated software is in use to optimize such pattern shift solution for a given blank and pattern.

Reference [96] is a recent example of how capable this technique is in practice. At the time of publication of this article, the intention is to have disclosed the idea of extended pattern shift [97]. In any case, such defect coverage technique requires very accurate position information of each ML-defect, relative to appropriate reference points on the mask blank, as discussed in Subsection 9.5.

9.5 Use of fiducial marks and limitations to the success of defect coverage

A mask blank is historically blank, and therefore, it only has its edges and corners as reference points. In view of the tolerance of 0.1 mm for a 152 mm substrate [98], these are too inaccurate to be used for precisely locating ML-defects for further mitigation. Fiducial marks are reference marks that can be patterned on purpose onto the blank in a stage before mask making [99, 100]. The position of blank defects is subsequently obtained relatively to these fiducial marks with high accuracy, in practice, in the range of 20–50 nm. These are also used as alignment marks for the mask writer with which the intended mask pattern is defined onto the blank. In this way, one can realize the solution calculated by the dedicated software mentioned in Subsection 9.4, at least within practical limits of uncertainty: (i) fiducial marks, themselves, have positional uncertainty, (ii) the estimation of the lateral size of the blank defect, together with its position, has a second uncertainty, and iii) the mask writer can have some alignment error. These three together will determine how a pattern shift solution found by software can be realized practically. Whether a solution exists will further depend on the specific pattern (pattern density also known as percentage of clear area, together with the distribution and range of feature sizes in the pattern, i.e. the so-called critical density [101]), and of course on the blank defects themselves (their number, size, position, estimated printing impact, …).

9.6 ML-defect mitigation by compensating for them

Apart from hiding the defects, as discussed in Subsection 9.4, ML-defect compensation is also considered a possibility. The expression 'compensation' of ML-defects inherently clarifies that the ML-defects are not specifically directly addressed to tweak the actual deficiency. Instead, one rather takes into account their presence and compensates for it, in this way avoiding that they will have an impact (within acceptable limits) on the pattern as printed on the wafer. This can be done either by intentional local re-design or repair in pattern data, done prior to mask writing (such as a inducing a small deviation of interconnect features [93]) to keep the printing impact of a defect below a certain threshold or by so-called absorber compensation repair. In the latter technique, the intended printed result of the pattern is (within limits) restored by locally editing the opaque features surrounding the ML-defect by opaque repair, in a way that this compensates for the presence of the ML-defect. This, in principle, can be done after mask patterning in a similar stage as the repair of absorber defects is done (see Section 8) and does not require fiducial marks as discussed in Subsection 9.5. The former technique is done during the design and requires

accurate defect information as discussed in the previous Subsection. Here, we will further address the latter.

Capability of compensation repair has been demonstrated to restore a process window for a defective location [102–107] and is illustrated in Figure 8. While this is essentially restoring the loss of local intensity, the phase contribution is not compensated, unless when the ML is locally edited [67].

One problem is that the determination of the compensation repair shape (which is removed from the absorber feature in the neighborhood of the ML-defect, as compensation for its presence) depends on information that is either not readily available or not independent from the illumination conditions used for wafer printing. The latter can yet be selected and used as input into a dedicated supporting simulation. The former is a bigger challenge.

Printability of an ML-defect depends on the propagation of the local distortion of the ML throughout its thickness, and that depends on the deposition conditions used for the ML (see smoothing in Subsection 9.2). Those parameters determine to what extent the distortion of the ML at the top of the ML-defect is, as it can be visualized, for example, by AFM (atomic force microscopy), propagates identically down to the substrate. Such typical smoothing parameters are not publicly known and, instead, most often unproven assumptions may be used.

If not available, the validity of the assumed propagation of the defect throughout the ML could be estimated by comparing the through-focus behavior as analyzed with an EUV-AIMS (discussed in Section 6) to simulations based on the assumptions made. Equally one can verify whether the derived compensation shape has the intended effect by similar analysis by EUV-AIMS after compensation repair.

As mentioned, it would be strongly preferred if the defect propagation through the ML could become accessible information for the mask shop that intends to use compensation repair with maximum capability and success rate. Transmission electron microscopy [108] can visualize that, but it is not in-line and rather a destructive metrology technique.

9.7 Lateral size-based limitation to either ML-defect mitigation technique

A statement made earlier is that the preference would be an economic availability of blanks without any printable ML-defects. If ML-defects are to some extent unavoidable, in the first place, it is vital to be able to detect them all (as discussed in Subsection 9.3). The lateral size of the ML-defects present is the basis for another essential

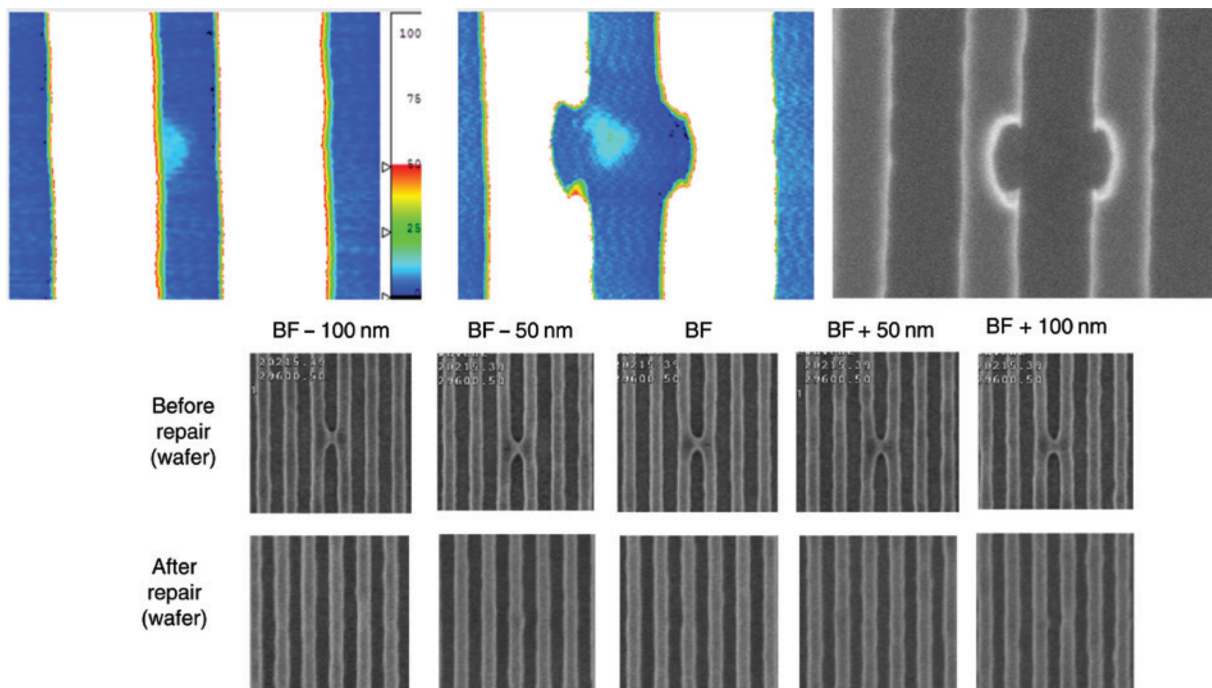

Figure 8: Illustration of absorber compensation as repair technique for ML-defects (repeated from Ref. [102]. Top from left to right: Top view by AFM before repair, respectively after repair, top view by SEM after repair (note that the ML-defect is not visible). Through-focus images are shown below, respectively, before and after repair, as indicated.

condition for their mitigation. If that exceeds the typical size of the opaque features in the intended absorber pattern to be patterned onto the blank, mitigation techniques as described in Subsections 9.4 and 9.6 may not be effective in avoiding (residual) printability. This is best explained in the example where the mask pattern consists merely of equal lines and spaces of a given half-pitch. In Figure 9 a half-pitch-dependent threshold for avoidance could be identified based on ABI intensity, above which a defect cannot be mitigated [89]. An earlier publication [109] visualizes the limitation for too 'solid' ML-defects based on direct qualifiers of an ML-defect. Only defects of a lateral size smaller than a half-pitch, possibly further reduced by the uncertainties on their exact position and size (as discussed in Subsection 9.5), can be overcome by compensation repair or pattern shift, respectively, discussed in Subsections 9.6 and 9.4. Defects exceeding half-pitch in lateral size must be totally avoided during blank manufacturing because, otherwise, no defect-free mask with such a line-and-space layout can be made. A similar reasoning can be made for arbitrary layouts. If the portion of the total pattern area is not critical, the intended half-pitch, the number of defects and their lateral size are not in proportion to each other, no solution for mitigation exists, and such mask (based on the given blank and intended pattern) cannot be made defect-free. Figure 10 illustrates the importance of each contribution toward (a high yield for) defect-free EUV masks.

10 Summary and conclusion

Most aspects of EUV mask defectivity will require further steps before full containment and readiness for high-volume manufacturing can be considered to be in place.

As the industry reports inferior capability to keep an EUV reticle free from frontside particles inside the EUV scanner than what the vendor claims as typical performance, frontside particles likely cannot be considered solved until a full-proof and high source power-compatible pellicle solution is established. The present pellicle solution is still gated to today's source power, and the clip-on frame solution, by its concept, is not likely a full-proof particle avoidance solution, as it may not provide integer zero probability for added particles because of the small gap between the pellicle frame and the reticle, to accommodate its use in a vacuum system. With the advent of EUV pellicles, handling, cleaning, and inspection must be proven to be compatible. The lack of actinic PMI that can do through-pellicle particle inspection is a second present major gap. Further, combining the optical, mechanical,

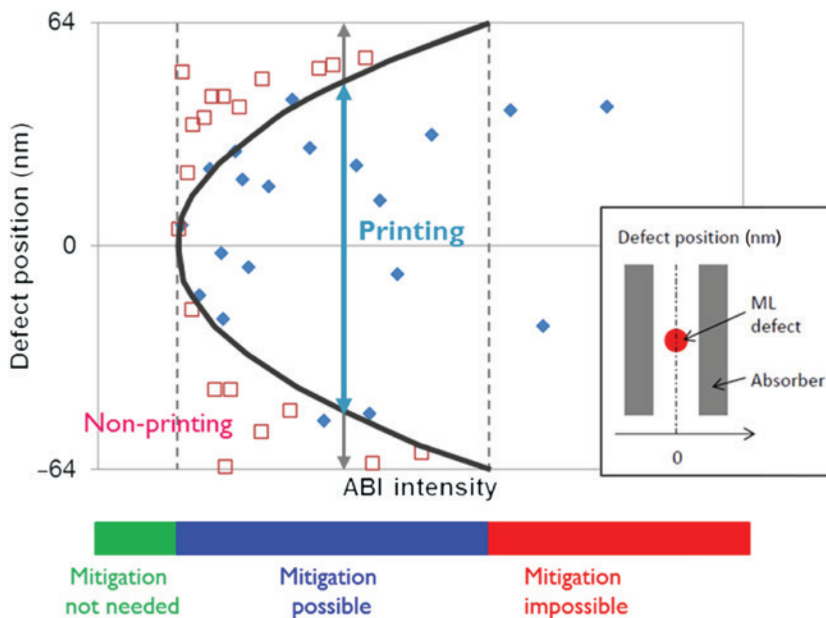

Figure 9: Dependence on ABI intensity and relative position of a defect to the line-and-space pattern of 16 nm hp (see inset), giving evidence for a boundary between printing and non-printing defects (adopted from Ref. [89]). Three zones can be derived based on ABI intensity. Small ABI intensity (green) does not print. For intermediate ABI intensity (blue), mitigation by covering defects by absorber makes them non-printable. For Large ABI intensity, coverage by a half-pitch absorber line is not possible, requiring a larger opaque (or non-critical) feature in the design to cover the defect.

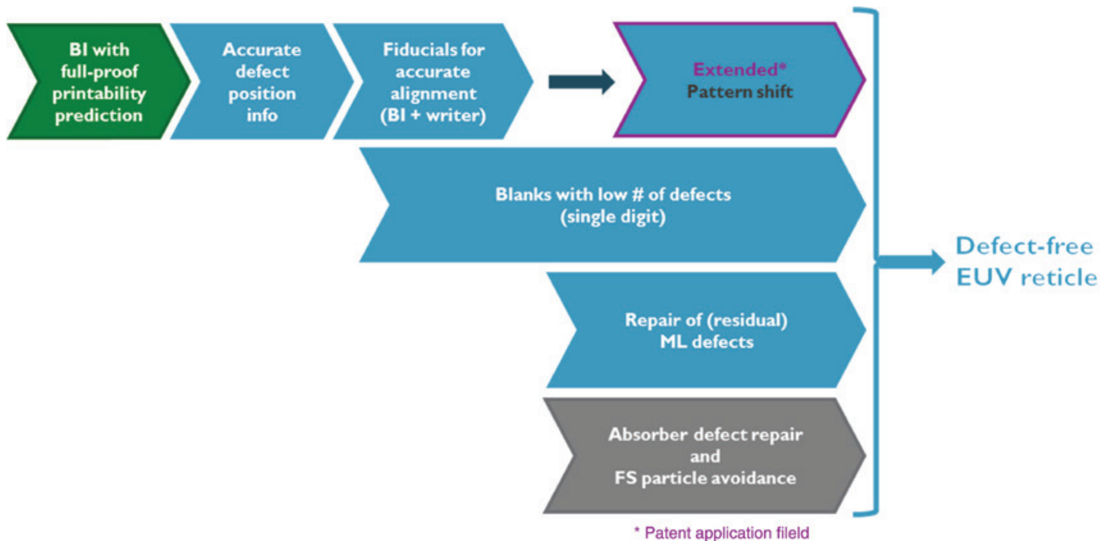

Figure 10: Schematic representation of the role of full-proof blank inspection, importance of accurate defect coordinates relative to blank fiducials, (extended) pattern shift and low number of ML-defects on a blank, each of them being collaborative pre-requisites for a sound solution for ML-defects. Also, contributions from other defect types discussed in earlier sections of this article are included (gray) as requirements for a fully defect-free mask.

and thermal requirements of a pellicle membrane into one solution shows an important challenge.

For backside particles, the message is perhaps the most positive. In principle, a tool set is available that facilitates appropriate inspection and a height-sensitive review capability to avoid overlay – and/or focus critical particles that can contaminate the backside of a reticle or, even worse, the reticle clamp.

How stable the performance of EUV reticles can be maintained over time in the situation of high source power remains to be seen. An infrastructure is underway that can investigate this in representative conditions of the HVM-oriented EUV scanner. Avoiding impact of repeated cleaning to the reticle frontside requires further attention. The cleaning media may still influence the capping layer and the upper part of the ML mirror and, even more easily, the unprotected sidewall of the ML-etched black border. ML-defects, as the most EUV-specific type of defects, establishes a real challenge unless the blank supply chain will be able to either fully solve the issue and supply defect-free blanks at high yield or fully support alternative mitigation that yet requires more than presently typically provided information by the blank vendor.

Acknowledgment: This invited article gives a review from an expert perspective. This personal viewpoint does not necessarily reflect a company opinion about the subject. Such expert opinion, when expressed to the community, as in the present article, could trigger dedicated discussion among professionals active in a similar field. This could lead to (even) more sound solutions than are presently already in place, under development, or, at least, under consideration. Logically, this published opinion builds on experience gathered on this subject as an employee of imec, based on the opportunities defined by the available tool set and on the network capabilities with external parties, as an independent R&D entity. A publication with a similar broad coverage of the different aspects of EUV mask defectivity and the availability of appropriate infrastructure was made by Liang in late 2015 [59] and is recommended as another expert review, from a different perspective.

References

[1] Steering Committee communication, Int. Symp. on EUV Lithography (2016).
[2] R. Jonckheere, F. Iwamoto, G. F. Lorusso, A. M. Goethals, K. Ronse, et al., Proc. SPIE 6730-12 (2007).
[3] R. Jonckheere, F. Iwamoto, G. F. Lorusso, A. M. Goethals and K. Ronse, in 'Int. Symp. on EUV Lithography' (2007).
[4] R. Jonckheere, T. Waehler, B. Baudemprez, U. Dietze, P. Dress, et al., Proc. SPIE 8352-0U (2012).
[5] SEMI standard E152.
[6] O. Brux, P. Dreß, H. Schmalfuß, R. Jonckheere, W. Koolen-Hermkens, et al., Proc. SPIE 8441-1J (2012).
[7] R. Jonckheere, B. Baudemprez, T. Waehler, D. Van den Heuvel, H. Schmalfuß, et al., in 'Int. Symp. on EUV Lithography' (2012).

[8] R. Jonckheere, D. van den Heuvel, B. Baudemprez, C. Jehoul and A. Pacco, in 'Int. Symp. on EUV Lithography' (2013).
[9] P. Jansen, D. Brouns, A. Bendiksen, P. Broman, E. Casimiri, et al., in 'Int. Symp. on EUV Lithography' (2016).
[10] B. Turkot, in 'Int. Symp. on EUV Lithography' (2016).
[11] Y. Hyun, in 'Int. Symp. on EUV Lithography' (2016).
[12] Y. Hyun, J. Kim, K. Kim, S. Koo, S. Kim, et al., Proc. SPIE 9422-1U (2015).
[13] D. Van den Heuvel, R. Jonckheere, B. Baudemprez, S. Cheng, G. Marcuccilli, et al., Proc. SPIE 8324-0L (2012).
[14] S. Mangan, R. Jonckheere, D. Van den Heuvel, M. Rozentsvige, V. Kudriashov, et al., Proc. SPIE 7823-2A (2010).
[15] R. Bonam, H.-Y. Tien, A. Chou, L. Meli, S. Halle, et al., Proc. SPIE 9776-1C (2016).
[16] S. Singh, S. Chen, T. Wähler, R. Jonckheere, T. Liang, et al., Proc. SPIE 7636-0Y (2010).
[17] T. Waehler, S. Singh, U. Dietze, R. Jonckheere and B. Baudemprez, in 'Int. Symp. on EUV', Lithography (2010).
[18] U. Dietze, P. Dress, T. Waehler, S. Singh, R. Jonckheere, et al., Proc. SPIE 7985-0N (2011).
[19] J. Choi, H. Lee, J. Yoon, T. Shimomura, A. Friz, et al., in 'Proc. SPIE 8166-1M' (2011).
[20] R. Jonckheere, D. Van den Heuvel, A. Pacco, I. Pollentier, B. Baudemprez, et al., Proc. SPIE 9256-0L (2014).
[21] S. Singh, D. Dattilo, U. Dietze, A. J. Kadaksham, I.-Y. Jang, et al., Proc. SPIE 8880-10 (2013).
[22] I.-Y. Jang, A. John, F. Goodwin, S.-Y. Lee, B.-G. Kim, et al., Proc. SPIE 9256-0I (2014).
[23] R. Jonckheere, E. Verduijn, G. Watanabe, N. Fukugami, Y. Sakata, et al., Proc. SPIE 9658-0H (2015).
[24] R. A. Claus, A. R. Neureuther, P. P. Naulleau and L. Waller, Proc. SPIE 9235-1A (2014).
[25] A. Vaglio Pret, R. Gronheid, T. R. Younkin, M. J. Leeson and P.-Y. Yan, Proc. SPIE 8322-0N (2012).
[26] T. Yamane, Y. Kim, N. Takagi, T. Terasawa, T. Ino, et al., Proc. SPIE 9256-0P (2014).
[27] R. Jonckheere, Y. Hyun, F. Iwamoto, B. Baudemprez, J. Hermans, et al., Proc. SPIE 6921-1W (2008).
[28] J. Hollenshead, L. Klebanoff, J. Vac. Sci. B 24, 118 (2006).
[29] J. Hollenshead, L. Klebanoff, J. Vac. Sci. B 24, 61 (2007).
[30] S. Bajt, H. N. Chapman, N. Nguyen, J. B. Alameda, J. C. Robinson, et al., Proc. SPIE 5037-236 (2003).
[31] U. Okoroanyanwu, A. Jiang, K. Dittmar, T. Fahr, et al., Proc. SPIE 7636-0H (2010).
[32] E. te Sligte, N. Koster, F. Molkenboer, P. van der Walle, P. Muilwijk, et al., Proc. SPIE 9985-20 (2016).
[33] D. Wack, Q. Q. Zhang, G. Inderhees and D. Lopez, Proc. SPIE. 7748-1Y (2010).
[34] I. Englard, Y. Cohen, Y. Elblinger, S. Attal, N. Berns, et al., Proc. SPIE 7272-28 (2009).
[35] S. H. Han, J. Na, W. Cho, D. H. Chung, C.-U. Jeon, et al., Proc. SPIE 7985-0V (2011).
[36] S. Mangan, C. C. Lin, G. Hughes, R. Brikman, A. Goldenshtein, et al., Proc. SPIE 8166-12 (2011).
[37] M. Malloy, B. Thiel, B. D. Bunday, S. Wurm, M. Mukhtar, et al., Proc. SPIE 9423-19 (2015).
[38] S. Iida, R. Hirano, T. Amano and H. Watanabe, J. Micro/Nanolithgr. MEMS MOEMS 15, 013510 (2016).
[39] http://semiengineering.com/19108/.
[40] Y. Ekinci, P. Helfenstein, R. Rajeev, I. Mochi, I. Mohacsi, et al., Proc. SPIE 9985-1P (2016).
[41] D. Hellweg, S. Perlitz, K. Magnusson, R. Capelli, M. Koch, et al., Proc. SPIE 9776-1A (2016).
[42] J. H. Peters, S. Perlitz, D. Hellweg and R. Capelli, in 'Int. Symp. on EUV Lithography' (2016).
[43] K. A. Goldberg, M. P. Benk, A. Wojdyla, D. G. Johnson and A. P. Donoghue, Proc. SPIE 9422-1A (2015).
[44] I. Mochi, K. A. Goldberg, R. Xie, P.-Y. Yan and K. Yamazoe, Proc. SPIE 7969-1X (2011).
[45] T. Harada, Y. Tanaka, T. Watanabe and H. Kinoshita, in 'Int. Symp. on EUV Lithography' (2013).
[46] S.-S. Kim, D. Lee, J. Park, E. Kim, C.-U. Jeon, et al., in 'Int. Symp. on EUV Lithography' (2013).
[47] C. Zoldesi, K. Bal, B. Blum, G. Bock, D. Brouns, et al., Proc. SPIE. 9048-1N (2014).
[48] D. Brouns, A. Bendiksen, P. Broman, E. Casimiri, P. Colsters, et al., Proc. SPIE 9776-1Y (2016).
[49] D. Brouns, this Journal.
[50] D. L. Goldfarb, Proc. SPIE 9635-0A (2015).
[51] E. Gallagher, J. Vanpaemel, I. Pollentier, H. Zahedmanesh, C. Adelmann, et al., Proc. SPIE 9635-0X (2015).
[52] I. Pollentier, J. Vanpaemel, J. U. Lee, C. Adelmann, H. Zahedmanesh, et al., Proc. SPIE 9776-20 (2016).
[53] J. U. Lee, J. Vanpaemel, I. Pollentier, C. Adelmann, H. Zahedmanesh, et al., Proc. SPIE 99850C (2016).
[54] I. Pollentier, C. Adelmann, C. Huyghebaert, J. U. Lee, M. Timmermans, et al., Proc. SPIE 10143 (2017) (in press).
[55] P. Jansen, M. Kamali, A. Kempa, R. Kox, R. de Kruif, et al., Proc. SPIE 9048-1N (2014).
[56] D. Brouns, Pellicle TWG, in 'SPIE-AL' (2016).
[57] J. Kruemberg, Pellicle TWG, in 'Int. Symp. on EUV Lithography' (2016).
[58] D. Dattilo, U. Dietze and J.-W. Hsu, Proc. SPIE 9635-1B (2015).
[59] T. Liang, J. Magana, K. Chakravorty, E. Panning and G. Zhang, Proc. SPIE 9635-09 (2015).
[60] D. L. Goldfarb, W. Broadbent, M. Wylie, N. Felix and D. Corliss, Proc. SPIE 9776-1H (2016).
[61] R. Jonckheere, F. Iwamoto, N. Stepanenko, A. M. Goethals and K. Ronse, 'Int. Symp. on EUV Lithography' (2008).
[62] M. Waiblinger, K. Kornilov, T. Hofmann and K. Edinger, Proc. SPIE 7545-0P (2010).
[63] T. Robinson, D. Yi, D. Brinkley, K. Roessler, R. White, et al., Proc. SPIE 8166-1J (2011).
[64] R. Jonckheere, D. Van Den Heuvel, F. Iwamoto, N. Stepanenko, A. Myers, et al., Proc. SPIE 7379-0R (2009).
[65] R. Jonckheere, D. Van den Heuvel, T. Bret, T. Hofmann, J. Magana, et al., Proc. SPIE 8166-0E (2011).
[66] A. Erdmann, P. Evanschitzky, T. Bret and R. Jonckheere, Proc. SPIE 8322-0E (2012).
[67] G. McIntyre, E. Gallagher, T. Robinson, A. C. Smith, M. Lawliss, et al., Proc. SPIE 8679-1I (2013).
[68] A. Barty, P. B. Mirkarimi, D. G. Stearns, D. W. Sweeney, H. N. Chapman, et al., Proc. SPIE. 4688-385 (2002).
[69] T. Onoue, T. Shoki, J. Horikawa, in 'Int. Symp. on EUV Lithography' (2016).
[70] P. Kearney, C. C. Lin, T. Sugiyama, H. Yun, R. Randive, et al., Proc. SPIE 7470-0X (2009).
[71] H. J. Kwon, R. Teki, J. Harris-Jones and A. Cordes, Proc. SPIE 8352-0X (2012).

[72] I.-Y. Kang, H.-S. Seo, B.-S. Ahn, D.-G. Lee, D. Kim, et al., Proc. SPIE 7636-1B (2010).
[73] V. Jindal, P. Kearney, J. Harris-Jones, A. Hayes and J. Kools, Proc. SPIE 7969-1A (2011).
[74] J.-P. Urbach, J. F. W. Cavelaars, H. Kusunose, T. Liang and A. R. Stivers, Proc. SPIE. 5256-556 (2003).
[75] W. Cho, P. A. Kearney, E. M. Gullikson, A. Jia, T. Tamura, et al., Proc. SPIE 6517-0D (2007).
[76] S. Stokowski, J. Glasser, G. Inderhees and P. Sankuratri, Proc. SPIE 76360Z (2010).
[77] K. Seki, T. Isogawa, M. Kagawa, S. Akima, Y. Kodera, et al., J. Micro/Nanolithgr. MEMS MOEMS 15, 021004 (2016).
[78] R. Jonckheere, D. Van den Heuvel, T. Abe, H. Hashimoto, C. Holfeld, et al., in 'Int. Symp. on EUV Lithography' (2009).
[79] D. Van den Heuvel, R. Jonckheere, J. Magana, T. Abe, T. Bret, et al., Proc. SPIE 7823-1T (2010).
[80] R. Jonckheere, D. Van den Heuvel, M. Lamantia, B. Baudemprez, E. Hendrickx, et al., in 'Int. Symp. on EUV Lithography' (2010).
[81] R. Jonckheere, D. Van den Heuvel, T. Bret, T. Hofmann, J. Magana, et al., Proc. SPIE 7985-0W (2011).
[82] T. Terasawa, T. Yamane, T. Tanaka, T. Iwasaki, O. Suga, et al., Proc. SPIE 7271-22 (2009).
[83] T. Suzuki, H. Miyai, K. Takehisa, H. Kusunose, T. Yamane, et al., Proc. SPIE 8441-15 (2012).
[84] H. Miyai, T. Suzuki, K. Takehisa, H. Kusunose, T. Yamane, et al, Proc. SPIE 8701-18 (2013).
[85] T. Murachi, T. Amano, T. Suzuki and H. Miyai, Proc. SPIE 9048-20 (2014).
[86] R. Jonckheere, D. Van den Heuvel, N. Takagi, H. Watanabe and E. Gallagher, Proc. SPIE 9422-16 (2015).
[87] N. Takagi, H. Watanabe, D. Van den Heuvel, R. Jonckheere and E. Gallagher, Proc. SPIE 9658-0F (2015).
[88] R. Jonckheere, N. Takagi, H. Watanabe, T. Yamane, D. Van den Heuvel, et al., in 'Int. Symp. on EUV Lithography' (2015).
[89] R. Jonckheere, T. Yamane, N. Takagi, H. Watanabe and C. Beral, in 'Int. Symp. on EUV Lithography' (2016).
[90] K. A. Goldberg, A. Barty, P. Seidel, K. Edinger, R. Fettig, et al., Proc. SPIE 6517-0C (2007).
[91] T. Yamane, T. Iwasaki, T. Tanaka, T. Terasawa, O. Suga, et al., Proc. SPIE 7379-0H (2009).
[92] J. Burns and M. Abbas, Proc. SPIE 78240 (2010).
[93] A. Elayat, P. Thwaite and S. Schulze, Proc. SPIE 8522-1W (2012).
[94] Z. J. Qi, J. H. Rankin, M. Lawliss, K. D. Badger and C. Turley, J. Micro/Nanolithgr. MEMS MOEMS 15, 023502 (2016).
[95] A. A. Kagalwalla and P. Gupta, J. Micro/Nanolithgr. MEMS MOEMS 13, 043005 (2014).
[96] G. Zhang, T. Liang, S. Satyanarayana, S. Misra, K. K. Chakravorty, et al., Proc. SPIE 9985-XX (2016).
[97] R. Jonckheere, Invited presentation at Photomask and Next Generation Lithography Mask Technology (Yokohama, April 5–7, 2017), to be published in Proc. SPIE.
[98] SEMI Standard P37, see http://www.semi.org/en/Standards.
[99] SEMI Standard P48, see http://www.semi.org/en/Standards.
[100] Pei-yang Yan, Proc. SPIE 7488-19 (2009).
[101] A. A. Kagalwalla, M. Lam, K. Adam and P. Gupta, Proc. ASP-DAC (2014).
[102] R. Jonckheere, T. Bret, D. Van den Heuvel, J. Magana, W. Gao, et al., Proc. SPIE 81661G (2011).
[103] T. Bret, R. Jonckheere, D. Van den Heuvel, C. Baur, M. Waiblinger, et al., Proc. SPIE8322-0C (2012).
[104] M. Waiblinger, R. Jonckheere, T. Bret, D. Van den Heuvel, C. Baur, et al., Proc. SPIE 8441-0F (2012).
[105] M. Waiblinger, T. Bret, R. Jonckheere and D. Van den Heuvel, Proc. SPIE 8522-1M (2012).
[106] D. Van den Heuvel, R. Jonckheere, T. Bret and M. Waiblinger, in 'Int. Symp. on EUV Lithography' (2012).
[107] A. Erdmann, P. Evanschitzky, T. Bret and R. Jonckheere, Proc. SPIE 8679-0Y (2013).
[108] J. Harris-Jones, E. Stinzianni, C. Lin, V. Jindal, R. Teki, et al., J. Micro/Nanolithgr. MEMS MOEMS 12, 013007 (2013).
[109] R. Jonckheere, D. Van den Heuvel, M. Lamantia, J. Hermans, E. Hendrickx, et al., 'Int. Symp. on EUV Lithography' (2009).

Rik Jonckheere
STS-AP, imec, Kapeldreef 75, Leuven 3001, Belgium
Rik.Jonckheere@imec.be

Rik Jonckheere is senior researcher mask technology in the Advanced Patterning Department at imec. He holds a Masters Degree in Solid-State Physics (1984). He joined imec in 1985 and has been working on e-beam direct write and experimental mask making. For 20 years he has been driving the interactions of imec's Advanced Lithography Program with the mask making community. Over the past 10 years his focus gradually has become EUV mask defectivity, its printability and its mitigation.